

Dynamic response of tube containing water subjected to impact loading

Original

Dynamic response of tube containing water subjected to impact loading / Moscoloni, C.; Kwon, Y. W.; Didoszak, J. M.; Mattiazzo, G.. - In: MULTISCALE AND MULTIDISCIPLINARY MODELING, EXPERIMENTS AND DESIGN. - ISSN 2520-8160. - 2:4(2019), pp. 281-290. [10.1007/s41939-019-00054-1]

Availability:

This version is available at: 11583/2837092 since: 2020-07-08T09:47:06Z

Publisher:

Springer

Published

DOI:10.1007/s41939-019-00054-1

Terms of use:

This article is made available under terms and conditions as specified in the corresponding bibliographic description in the repository

Publisher copyright

Springer postprint/Author's Accepted Manuscript

This version of the article has been accepted for publication, after peer review (when applicable) and is subject to Springer Nature's AM terms of use, but is not the Version of Record and does not reflect post-acceptance improvements, or any corrections. The Version of Record is available online at: <http://dx.doi.org/10.1007/s41939-019-00054-1>

(Article begins on next page)

Multiscale and Multidisciplinary Modeling, Experiments and Design

Dynamic Response of Tube Containing Water Subjected to Impact Loading

--Manuscript Draft--

Manuscript Number:	MMED-D-19-00030
Full Title:	Dynamic Response of Tube Containing Water Subjected to Impact Loading
Article Type:	Original Paper
Funding Information:	
Abstract:	<p>Dynamic response of a round aluminum tube supported at both ends was investigated when impacted at its center by an external mechanical loading. The tube was subjected to different conditions. First, the empty tube was tested. Then the tube was filled with different amounts of stationary water (i. e. 25%, 50%, 75% and 100% full), based on the inner volume of the tube. Finally, flowing water through the tube was considered. Different magnitudes of impact loading were also applied. The study was primarily conducted experimentally with some additional numerical studies completed to further understand the results. The impact force as well as strain along the tube were measured for all described test conditions. Their results were compared. Additionally, the vibrational frequency and damping of the system were examined using strain-time histories. The results showed that the dynamic behavior of the tube was significantly dependent on the amount of internal water as well as its flow condition.</p>
Corresponding Author:	Claudio Moscoloni Politecnico di Torino ITALY
Corresponding Author Secondary Information:	
Corresponding Author's Institution:	Politecnico di Torino
Corresponding Author's Secondary Institution:	
First Author:	Claudio Moscoloni
First Author Secondary Information:	
Order of Authors:	Claudio Moscoloni
	Young W. Kwon
	Jarema M. Didoszak
	Giuliana Mattiazzo
Order of Authors Secondary Information:	
Author Comments:	
Suggested Reviewers:	

[Click here to view linked References](#)

Dynamic Response of Tube Containing Water Subjected to Impact Loading

C. Moscoloni^{1,2}, Y. W. Kwon^{1,*}, J. M. Didoszak¹ and G. Mattiazzo²

¹Dept. of Mechanical & Aerospace Engineering
Naval Postgraduate School
Monterey, CA 93943, USA

²Dept. of Mechanical & Aerospace Engineering
Politecnico di Torino
Turin, Italy

Corresponding author: * E-mail) ywkwon@nps.edu

Keywords. Fluid structure interaction, Impact loading, Vibration, Pipe with fluid, Dynamic analysis

1
2
3
4 **Abstract**
5

6 Dynamic response of a round aluminum tube supported at both ends was investigated when
7 impacted at its center by an external mechanical loading. The tube was subjected to different
8 conditions. First, the empty tube was tested. Then the tube was filled with different amounts of
9 stationary water (i. e. 25%, 50%, 75% and 100% full), based on the inner volume of the tube.
10
11 Finally, flowing water through the tube was considered. Different magnitudes of impact loading
12 were also applied. The study was primarily conducted experimentally with some additional
13 numerical studies completed to further understand the results. The impact force as well as strain
14 along the tube were measured for all described test conditions. Their results were compared.
15
16 Additionally, the vibrational frequency and damping of the system were examined using strain-
17 time histories. The results showed that the dynamic behavior of the tube was significantly
18 dependent on the amount of internal water as well as its flow condition.
19
20
21
22
23
24
25
26
27
28
29
30
31
32
33
34
35
36
37
38
39
40
41
42
43
44
45
46
47
48
49
50
51
52
53
54
55
56
57
58
59
60
61
62
63
64
65

Introduction

Tubes and pipes are common in many industrial applications. Most have a round shape and contain fluid either inside and/or surrounding them, depending on the application. As a result, there has been extensive research on dynamic motion of tubes and pipes carrying fluids. For example, Flow-Induced Vibration (FIV) has been investigated extensively. [1-4].

Vibration of a fluid-transporting pipe was studied in the early 1950's [5, 6]. Since then much more research has been completed. Later researchers considered instability of a pipe depending on different end supports, steady and unsteady flows, straight or curved pipes, etc. A good summary of this subsequent research was published in Ref. [7, 8]. While those particular studies focus on the internal flow of a pipe, there is also research in external flow over a pipe such as Vortex-Induced Vibrations (VIV). Some of the latter works are given in Refs. [9-12].

However, not all of those papers considered mechanical impact loading of the pipe. Impact studies on circular cylinders were conducted in Refs. [13, 14]. One paper developed an analytical solution of a simply supported orthotropic cylindrical shell subjected to lateral impact loading [13] while the other investigated structural coupling of two concentric composite circular cylinders containing fluid inside their annulus and subjected to impact loading [14].

The objective of this study is to investigate the dynamic response of a round tube containing either stationary or moving fluid while supported at both ends and impacted at the center between the supports. The subsequent section describes the experimental set-up and test procedures. Finally, the results and discussion are provided, followed by conclusions.

Description of Experiments

A round aluminum alloy tube was used for this study. The tube has a 25.4 mm OD and 1.0 mm thickness. The tube was supported at both ends as shown in Figure 1(a). The support structure was fabricated using a 3-D printer with polylactide as seen in Figure 1(b). The tube was inserted into each support. Fitted snugly, a set screw at the top of the support structure was used to hold the tube in place. The overall height of the support was 155.6 mm, with a base width of 110 mm and a 50 mm depth. The mounting holes and set screw hole have a common diameter of 6 mm. The unsupported length of the beam between the two supports was 0.762 m. Eleven equally spaced strain gages were attached along the length of the beam in order to measure its longitudinal strain. Starting with the gage placed at the center of the tube's length, additional gages were placed at equal intervals of 70 mm in both directions, to the right and left of center. The axial strain gages were attached opposite to the side of impact on the tube diameter.

The tube was tested in various conditions. The base condition consisted of the dry tube which did not contain any fluid inside. The next set of cases included varying amounts of stationary water inside the tube. In terms of the inside volume of the tube, the water levels were set to 25%, 50%, 75%, and 100%, respectively. Both ends of the tube were sealed by a rubber laboratory stopper to retain the water inside of the tube during the tests. The final case considered steady-state water flow through the pipe. The Reynolds number of the flow rate using a water pump was calculated as 5.21×10^5 based on the inner diameter of the tube.

Impact loading was applied to the tube using a pendulum motion and the striking apparatus shown in Figure 2. The impact pendulum had a mass of 2.15 kg and was supported at the top with a frictionless bearing. The length of the pendulum as measured from the top bearing support to the bottom hemispherical impactor was 0.50 m. A load cell was attached behind the hemispherical

1
2
3
4
5
6
7
8
9
10
11
12
13
14
15
16
17
18
19
20
21
22
23
24
25
26
27
28
29
30
31
32
33
34
35
36
37
38
39
40
41
42
43
44
45
46
47
48
49
50
51
52
53
54
55
56
57
58
59
60
61
62
63
64
65

impactor to measure the impact force. The magnitude of the impact loading was varied by changing the initial angle of the pendulum. The angle was set to zero when the pendulum lay in the vertical position such that the impactor was just barely in contact with the tube. As the impactor was raised, the desired angle was set. The typical impact angle was 45°, however, the angle was also varied to the angles of 30° and 60°.

Each test case was repeated ten times to ensure repeatability of the test results. During each test, the impact force and strain data were recorded at a data sampling frequency of 1000 Hz. This rate was selected to make sure that sufficient data was collected for accurate measurement of the primary vibrational frequency of the tube.

Results and Discussion

Figure 3 shows three impact force time-histories at the same condition to check the repeatability of the test result. Even though at least ten tests were conducted for each condition, only three tests were plotted not to overcrowd the plots. They were all found to be consistent as shown in the figure. As a result, the following discussion presents only a single typical test result for every test case rather than averaging the ten test results.

The first case examined was the base case, which consisted of a tube without any fluid, i.e. the dry tube. Figure 4 shows the impact force as well as strain gage responses at selected locations. The impact force was applied with the initial angle 45° . The impact event was completed by 13 msec. The impact force shows high frequency oscillations with a peak force of 88 N. Such oscillation is considered to be a result of the localized dynamic deformation of the tube at the contact location due to the relatively thin wall thickness of the tube at only 1.0 mm thick. These high frequency components were not observed in prior tests where such local deformation was not possible.

Strain plots for five selected positions along the length of the tube are also included in Figure 4. Strain gage locations are denoted as left (L), right (R) plus a number from 1-5. Figure 2 depicts these positions along the length of the tube with L1 being nearest to the impact point and L5 closest to the end support on the left side of tube. The enumeration pattern is mirrored on the right side of the tube, while C indicates the center location opposite the impact point.

The maximum tensile strain of 1.12×10^{-3} m/m occurred at the center strain gage location. In general, tensile strain was found to decrease with an increase in distance from the tube center span location while compressive strain increased as the gage location approached the supported end. A maximum compressive strain of 4.62×10^{-4} m/m was observed at the 'L5' strain gage which

1
2
3
4 was located very near to one of the supported ends. This strain characteristic suggests that the 3-D
5
6 printed support provided the bending moment to the tube as expected. However, the support did
7
8 not provide a fully clamped condition because the support structure was not completely rigid. The
9
10 tube was inserted snugly into the cylindrical opening of the support structure, but not otherwise
11
12 fixed in place, with the exception of a 6mm set screw at each end support. The strain responses
13
14 were symmetric in terms of the tube center.
15
16
17
18

19 Figure 5 shows a longer time history of strain at the center. The plot shows the free
20
21 vibration of the tube after the impact loading has ended. The vibrational frequency was determined
22
23 from the strain response using the Fast Fourier Transform (FFT). The frequency was 143 Hz. From
24
25 the beam theory, the tube had a frequency of 119 Hz for simply supported ends and 270 Hz in the
26
27 case with clamped ends. Thus, this also suggests that the actual support condition was partially
28
29 clamped.
30
31
32

33 In order to represent the actual boundary condition as in the experimental set-up, a torsional
34
35 spring was attached to a simply supported tube beam structure. When the torsional spring is zero,
36
37 the tube is simply supported, while it is fully clamped when the torsional spring is infinite or very
38
39 stiff. The experimental investigation thus falls between these two boundary conditions. When a
40
41 torsional spring of 6300 N-m was used in the model, the frequency from the Finite Element
42
43 Analysis (FEA) using 40 beam elements resulted in 143 Hz which matched the experimental
44
45 frequency. All subsequent FEA used the same torsional springs at the boundary condition.
46
47
48
49

50 The next test was conducted for the tube at 100% full and with stationary water. The
51
52 interior of the tube was filled with water, and both ends of the tube were sealed. The impact force
53
54 and strains are plotted in Figure 6 for the 45° impact angle. As compared to the response without
55
56 water, the tube full of water had a greater impact force and larger strains along the tube. The peak
57
58
59
60
61
62
63
64
65

1
2
3
4 impact force was 70% greater than the dry case, and the peak force occurred earlier in the full
5
6 water case. The strain at the center increased by 58% resulting from the water contained inside of
7
8 the tube. Even though the magnitude of such an increase is different from gage to gage, the general
9
10 characteristics of the strain curves remained almost the same between the dry tube and the one full
11
12 of water.
13
14

15
16 The change in maximum force and strain is plotted in Figure 7 as a function of the amount
17
18 of stationary water inside the tube. The increment was varied by 25% of the volume. The impact
19
20 condition was the same for all water amounts tested. The results show that the magnitude of the
21
22 peak impact force was approximately linear to the water level. However, the peak strain at the
23
24 center of the tube varied in a step-wise shape. The strain remained almost constant from 25% to
25
26 75% water levels. Strains at the gage 'L2' showed a larger increase from no water to the 25% water
27
28 case, and the increase became much less from the 25% water level. Other gages showed roughly
29
30 a linear variation of the peak strains in terms of the water level.
31
32
33

34
35
36 Vibrational frequencies were computed from the strain measurements as in the case of the
37
38 dry tube. The addition of internal water reduced the vibrational frequency as shown in Figure 8.
39
40 The reduction in strain was more or less linear with the increase of water level. The natural
41
42 frequency of the beam was also computed using the FEA. As discussed above, a torsional spring
43
44 was attached to a simply supported end to represent the actual boundary condition in the
45
46 experimental test set-up. Water was added to the mass of the tube, or in other words, the tube had
47
48 a greater mass depending on the water level but its stiffness did not change. The numerical results
49
50 are also plotted in Figure 8. This result was labeled as 'Numerical w/ mass'. The numerical
51
52 solutions show a larger decrease in the frequency than the experimental data with increasing water
53
54 level. For example, when the tube was full, the numerical frequency was about 20% lower than
55
56
57
58
59
60
61
62
63
64
65

1
2
3
4 the experimental frequency. This is because the effect of water on the stiffness of the tube was
5
6 completely ignored in the numerical model.
7
8

9 The stiffness of the tube was modified resulting from the internal water addition as such

$$EI_n = EI(1 + f_w) \quad (1)$$

10
11 where EI is the tube rigidity, EI_n is the new rigidity of the tube with the effect of internal water,
12
13 and f_w is the fraction of water level which varies from 0 to 1. The new finite element results are
14
15 also compared in Figure 8. The numerical solutions using Equation (1) compared well to the
16
17 experimental data. Equation (1) is a very simple modification of the pipe stiffness resulting from
18
19 the static water inside. This equation needs further assessment and may require a modification to
20
21 be applicable to different tubes and fluids. However, this equation suggests that internal fluid
22
23 influences not only the effective mass but also effective stiffness of a tube containing a fluid.
24
25
26
27
28
29
30
31

32
33 Figure 9 compares the peak force values among three different cases as a function of the
34
35 initial impact condition. The three cases were the tube without water, 100% stationary water, and
36
37 fully flowing water, respectively. The impact condition was varied in terms of the initial height of
38
39 the impactor. The left figure of Figure 9 was plotted in terms of the initial height while the right
40
41 figure of Figure 9 was plotted in terms of the square root of the initial height. The initial height is
42
43 proportional to the initial potential energy of the impact, and the square root of the initial height is
44
45 proportional to the initial impact velocity.
46
47
48
49

50 As expected, the peak impact force increased along with the initial height. Internal water,
51
52 whether stationary or flowing, increased the impact force as well. The difference between the
53
54 stationary and flowing water cases was minor for the peak impact force. When the peak force was
55
56 plotted for the square root of the initial height, the former was almost linear to the latter for the
57
58 flowing water case. In other words, the peak impact velocity was linearly proportional to the initial
59
60
61
62
63
64
65

1
2
3
4 impact velocity. The stationary water case was similar to the flowing water case. However, the dry
5
6 tube showed a nonlinear behavior between the impact force and impact height.
7
8

9 The maximum strain at the center of the tube is plotted in Figure 10 as a function of the
10
11 initial height as before. The strain of the tube with flowing water showed a linear relationship
12
13 between the maximum strain and the impact velocity. However, the tube without and with full
14
15 stationary water did not show such a linear relationship. Even though the peak impact force was
16
17 similar between the stationary and flowing water, the maximum strain at the center was not close
18
19 when the initial height was 0.15 m.
20
21
22

23 The vibrational frequency of the tube with flowing water was 81 Hz, which is lower than
24
25 the frequency of the tube without and with stationary water. The experimental frequency with
26
27 flowing water was very close to the numerical frequency of the dry tube while the water mass was
28
29 added to the tube mass without any modification of its stiffness. The stationary water contributed
30
31 the effective tube stiffness and mass while the flowing water only contributed to the effective mass
32
33 in terms of the vibrational frequency.
34
35
36
37

38 Damping of the vibration was measured using the logarithmic decrement. Free vibration at
39
40 the center of the tube after completion of the impact, as shown in Figure 5, was used to compute
41
42 the logarithmic decrement. The first three peaks just after impact were averaged for the logarithmic
43
44 decrement value, which was plotted in Figure 11 for various levels of stationary water inside the
45
46 tube. The results showed an increase in the logarithmic decrement as a function of the water level.
47
48 When the tube was full of stationary water, the logarithmic decrement was more than two times
49
50 greater than that of the dry tube. On the other than, when water was flowing inside the tube, the
51
52 logarithmic decrement was only about 30% greater than that of the dry tube. That is, stationary
53
54 water resulted in much greater damping than did the flowing water.
55
56
57
58
59
60
61
62
63
64
65

1
2
3
4
5
6
7
8
9
10
11
12
13
14
15
16
17
18
19
20
21
22
23
24
25
26
27
28
29
30
31
32
33
34
35
36
37
38
39
40
41
42
43
44
45
46
47
48
49
50
51
52
53
54
55
56
57
58
59
60
61
62
63
64
65

Conclusions

Dynamic motions of a tube were studied when the tube was filled to varying levels of fullness based on internal volume of stationary water as well as with flowing water. The dynamic response was measured using strain gages attached along the length of the tube while it was impacted using a pendulum motion. The impact force was also recorded. The stationary water level inside the tube influenced the dynamic motion of the tube significantly. Both impact loading and the resultant strains increased along with the water level as the initial impact condition remained the same. The peak impact force as well as the maximum strain at the center increased more than 50% when the tube was full of stationary water as compared to the no water case.

The peak impact force was more or less similar between the full stationary and flowing water cases. However, the tube response was not necessarily similar between the two cases. For example, the vibrational frequency was quite different depending on whether or not the water was stationary or flowing. The former case had 20% greater frequency than the latter case. As a result, the strain responses were also different.

A numerical study was conducted to model the vibration of the tube. In order to simulate the actual boundary condition of the physical experiment, a torsional spring was attached to each end while the tube was simply supported at each end. If the torsional spring constant is zero, the boundary is simply supported. If the spring constant is very large, i.e. infinite, the boundary condition is clamped. The actual boundary condition was between these two extreme cases, i.e. partially clamped. With the proper selection of a spring constant, the numerical model gave a frequency which agreed very well with the experimentally measured value.

The numerical model was run for the tube with water using the properly adjusted boundary condition. The internal water was added to the tube water in the numerical model to modify the

1
2
3
4 density of the tube. When the stiffness of the tube was modified with the stationary water, the
5
6 results agreed better with the experimental frequency. On the other hand, the numerical frequency
7
8 with flowing water was better without modification of the tube stiffness.
9

10
11 Damping resulting from the internal water increased with the addition of stationary water.
12
13 However, the flowing water case resulted in lower damping than the stationary water. In
14
15 conclusion, the amount of stationary internal water as well as flowing water greatly influenced the
16
17 dynamic behavior of the tube subjected to external impact loading.
18
19
20
21
22
23
24
25
26
27
28
29
30
31
32

33 **Acknowledgements**

34
35 This work was supported by Office of Naval Research (ONR), and the Program Manager is Dr.
36
37 Yapa Rajapakse.
38
39
40
41

42 **Conflict of Interest Statement**

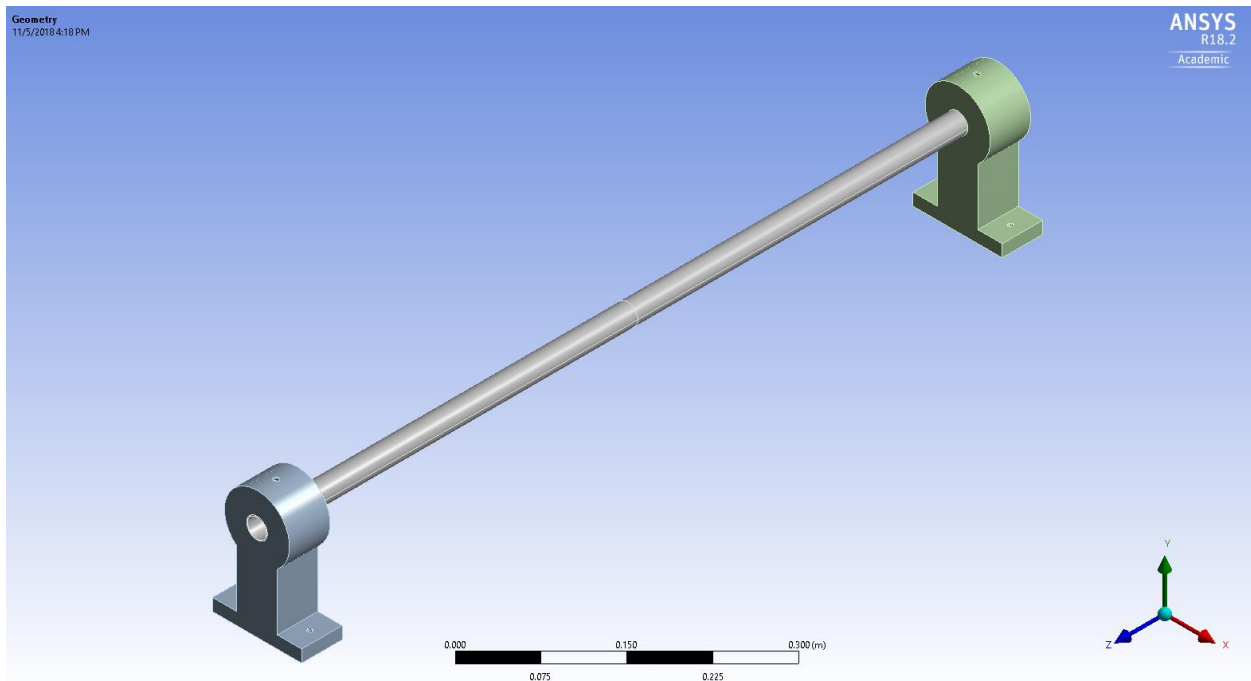
43
44 On behalf of all authors, the corresponding author states that there is no conflict of interest.
45
46
47
48
49
50
51
52
53
54
55
56
57
58
59
60
61
62
63
64
65

References

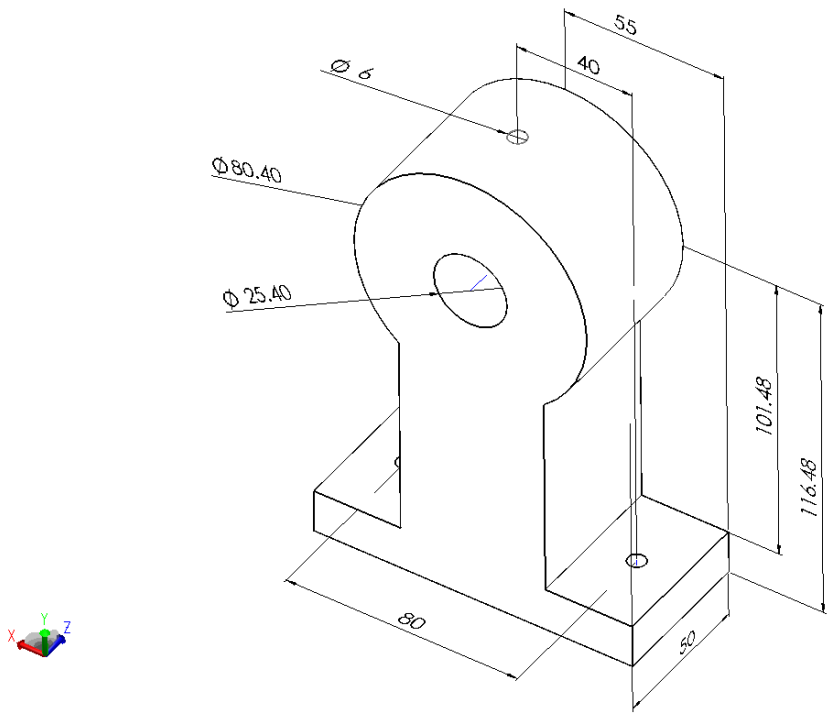
- [1] Blevin RD (1994), Flow-Induced Vibration, 2nd ed., Krieger Publishing Co., Malabar, Florida.
- [2] Naudascher E, Rockwell D (2005), Flow-Induced Vibrations: An Engineering Guide, Dover Publications, Inc., Mineola, New York.
- [3] Kaneko S, Nakamura T, Inada F, Kato M, Ishihara K, Nishihara T, Mureithi NW, Langthjem MA (2014), Flow-Induced Vibrations: Classifications and Lessons from Practical Experiences, 2nd ed., Elsevier, Amsterdam, Netherlands.
- [4] Weaver DS, Ziada S, Au-Yang, M, Chen SS, Paidoussis MP, Pettigrew MJ (2000), “Flow-Induced Vibrations in Power and Process Plant Components—Progress and Prospects”, Journal of Pressure Vessel Technology, Vol. 22, August, pp. 339-348.
- [5] Ashley H, Haviland G (1950), “Bending Vibration of a Pipe Line Containing Flowing Fluid”, Journal of Applied Mechanics, Vol. 17, pp. 229-232.
- [6] Housner GW (1952), “Bending Vibrations of a Pipe When Liquid Flows through It”, Journal of Applied Mechanics, Vol. 19, pp. 205-208.
- [7] Paidoussis MP (1987), “Flow-Induced Instabilities of Cylindrical Structures”, Applied Mechanics Review, Vol. 40, pp. 163-175.
- [8] Shuajin Li, B. W. (2015). FSI reasearch in pipeline systems - A review of the literature. Journal of Fluids and Structures.
- [9] Chen SS (1986), “A Review of Flow-Induced Vibration of Two Circular Cylinders in Crossflow”, Journal of Pressure Vessel Technology, Vol. 108, No. 4, pp. 382-393.
- [10] Au-Yang MK, Blevins RD, Mulcahy TM (1991), “Flow-Induced Vibration Analysis of Tube Bundles—A Proposed Section III Appendix N Nonmandatory Code”. Journal of Pressure Vessel Technology, Vol. 113, No. 2, pp. 257-267.

- 1
2
3
4 [11] Griffin OM (1980), “Vortex-Excited Cross-Flow Vibrations of a Single Cylindrical Tube”,
5
6 Journal of Pressure Vessel Technology, Vol. 102, No. 2, pp. 158-166.
7
8
9 [12] Weaver DS, Ziada S, Au-Yang MK, Chen SS, Paidoussis MP, Pettigrew MJ (2000), “Flow-
10
11 Induced Vibrations in Power and Process Plant Components—Progress and Prospects”,
12
13 Journal of Pressure Vessel Technology, Vol. 122, August, pp. 339-348.
14
15
16 [13] Christoforou AP, Swanson SR (1990), "Analysis of Simply-Supported Orthotropic
17
18 Cylindrical Shells Subject to Lateral Impact Loads.", Journal of Applied Mechanics, Vol. 57,
19
20 No. 2, pp. 376-382.
21
22
23 [14] Alaei D, Kwon YW, Ramezani A (2019), “Fluid-Structure Interaction on Concentric
24
25 Composite Cylinders Containing Fluids in the Annulus”, Multiscale and Multidisciplinary
26
27 Modeling, Experiments, and Design, <https://doi.org/10.1007/s41939-019-00044-3>
28
29
30
31
32
33
34
35
36
37
38
39
40
41
42
43
44
45
46
47
48
49
50
51
52
53
54
55
56
57
58
59
60
61
62
63
64
65

1
2
3
4
5
6
7
8
9
10
11
12
13
14
15
16
17
18
19
20
21
22
23
24
25
26
27
28
29
30
31
32
33
34
35
36
37
38
39
40
41
42
43
44
45
46
47
48
49
50
51
52
53
54
55
56
57
58
59
60
61
62
63
64
65



(a) Tube supported at both ends



(b) 3-D printed support structure

Figure 1. Tube supported at both ends with detailed figure of the support structure.

1
2
3
4
5
6
7
8
9
10
11
12
13
14
15
16
17
18
19
20
21
22
23
24
25
26
27
28
29
30
31
32
33
34
35
36
37
38
39
40
41
42
43
44
45
46
47
48
49
50
51
52
53
54
55
56
57
58
59
60
61
62
63
64
65

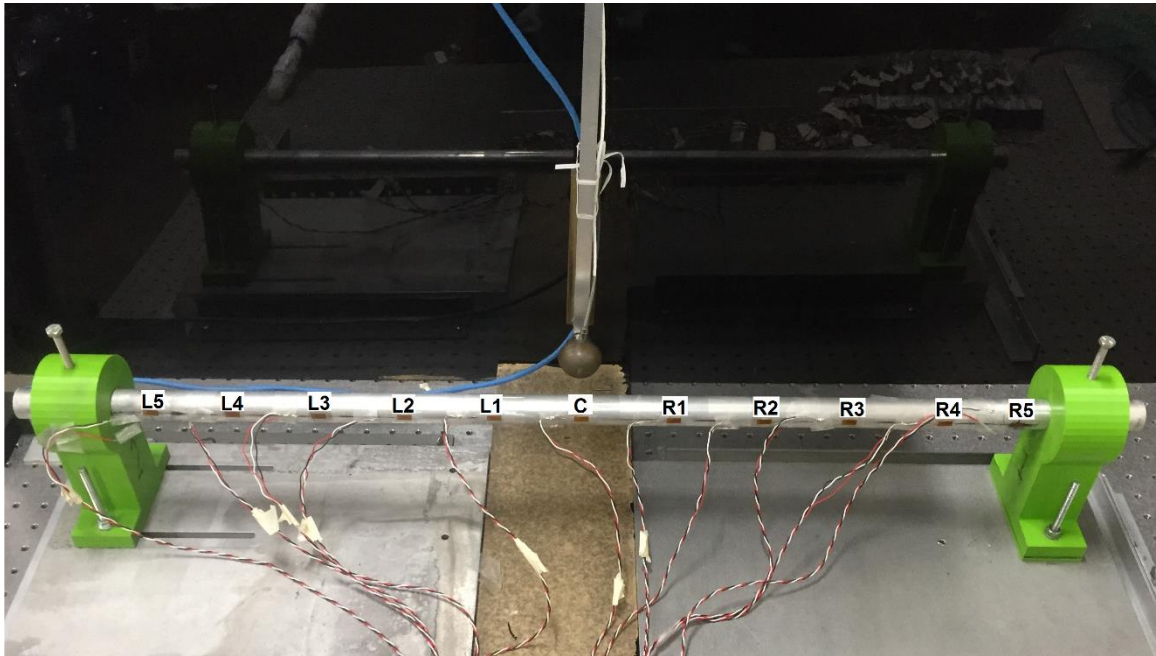


Figure 2. Impact pendulum and tube with strain gage locations

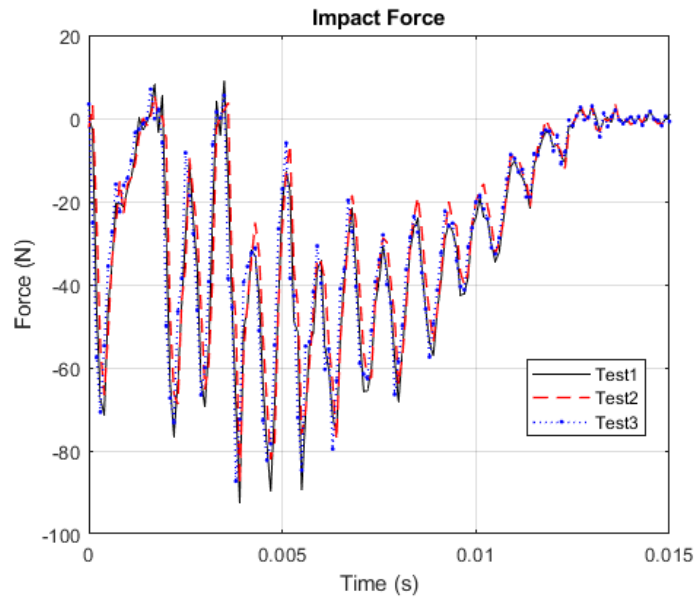


Figure 3. Repeated impact force time-history

1
2
3
4
5
6
7
8
9
10
11
12
13
14
15
16
17
18
19
20
21
22
23
24
25
26
27
28
29
30
31
32
33
34
35
36
37
38
39
40
41
42
43
44
45
46
47
48
49
50
51
52
53
54
55
56
57
58
59
60
61
62
63
64
65

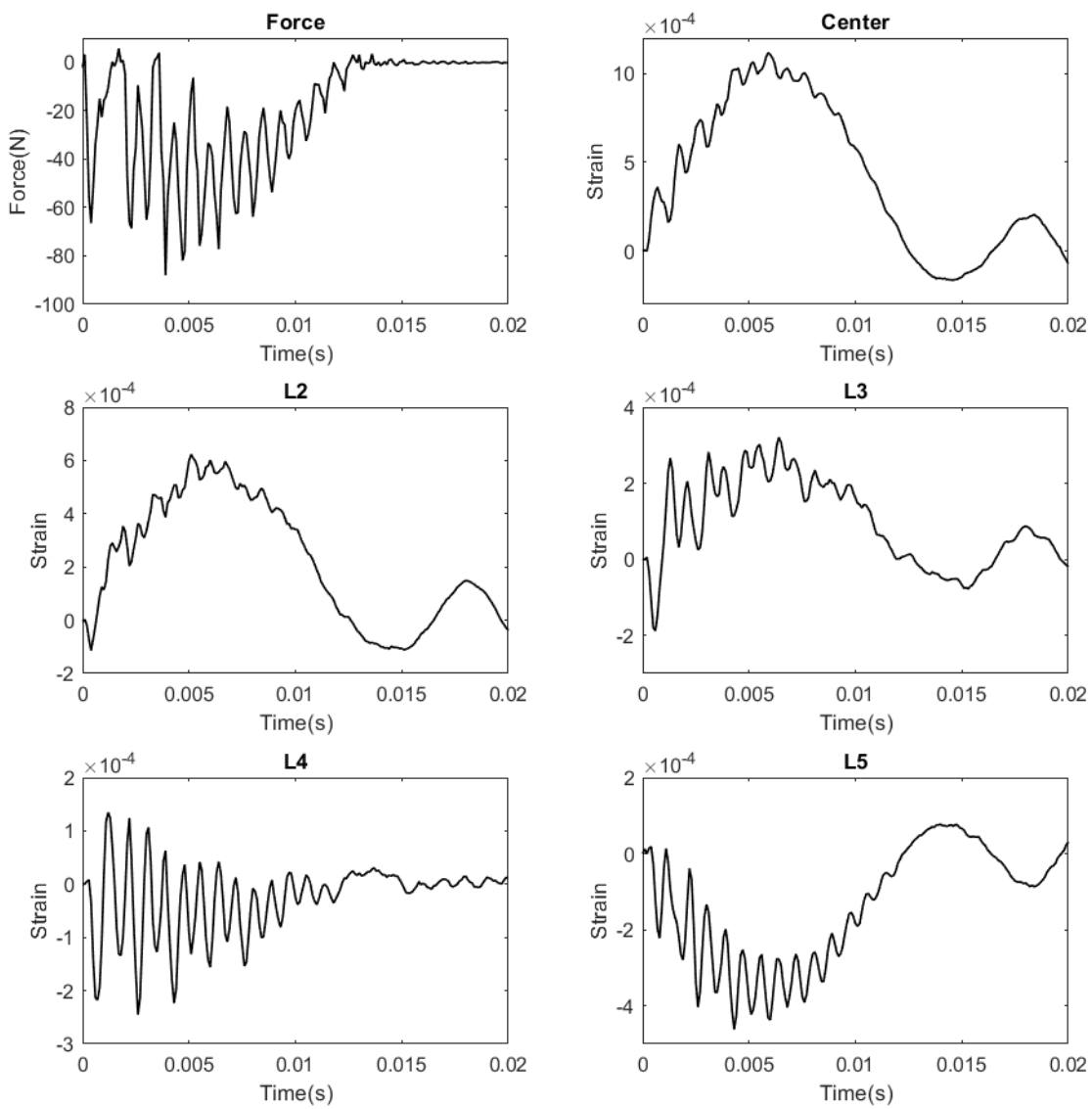


Figure 4. Impact force and strain plots for the dry tube

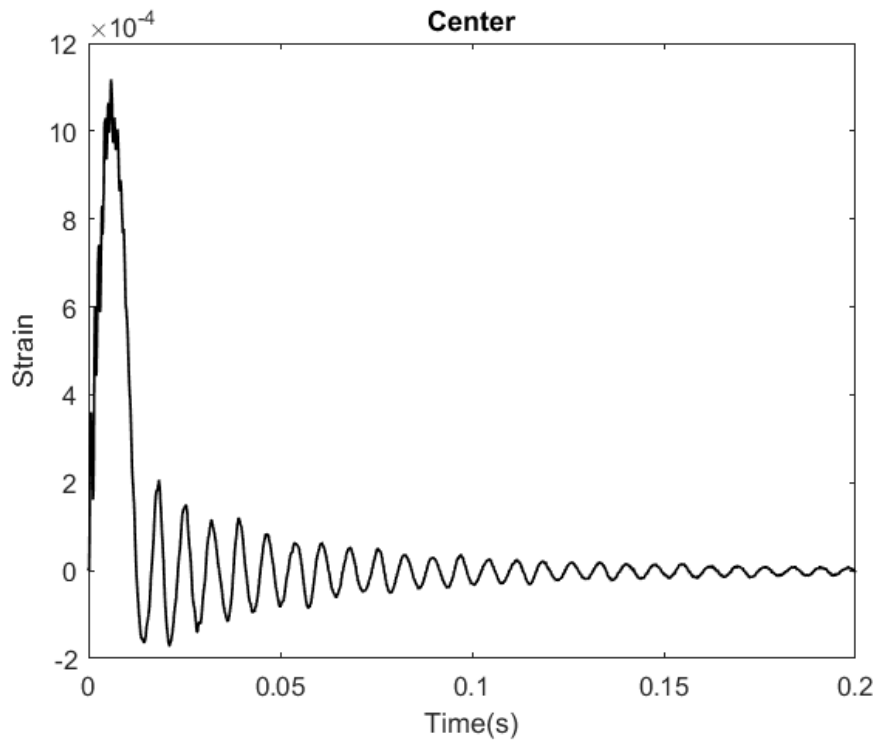


Figure 5. Strain plot at the center of the dry tube

1
2
3
4
5
6
7
8
9
10
11
12
13
14
15
16
17
18
19
20
21
22
23
24
25
26
27
28
29
30
31
32
33
34
35
36
37
38
39
40
41
42
43
44
45
46
47
48
49
50
51
52
53
54
55
56
57
58
59
60
61
62
63
64
65

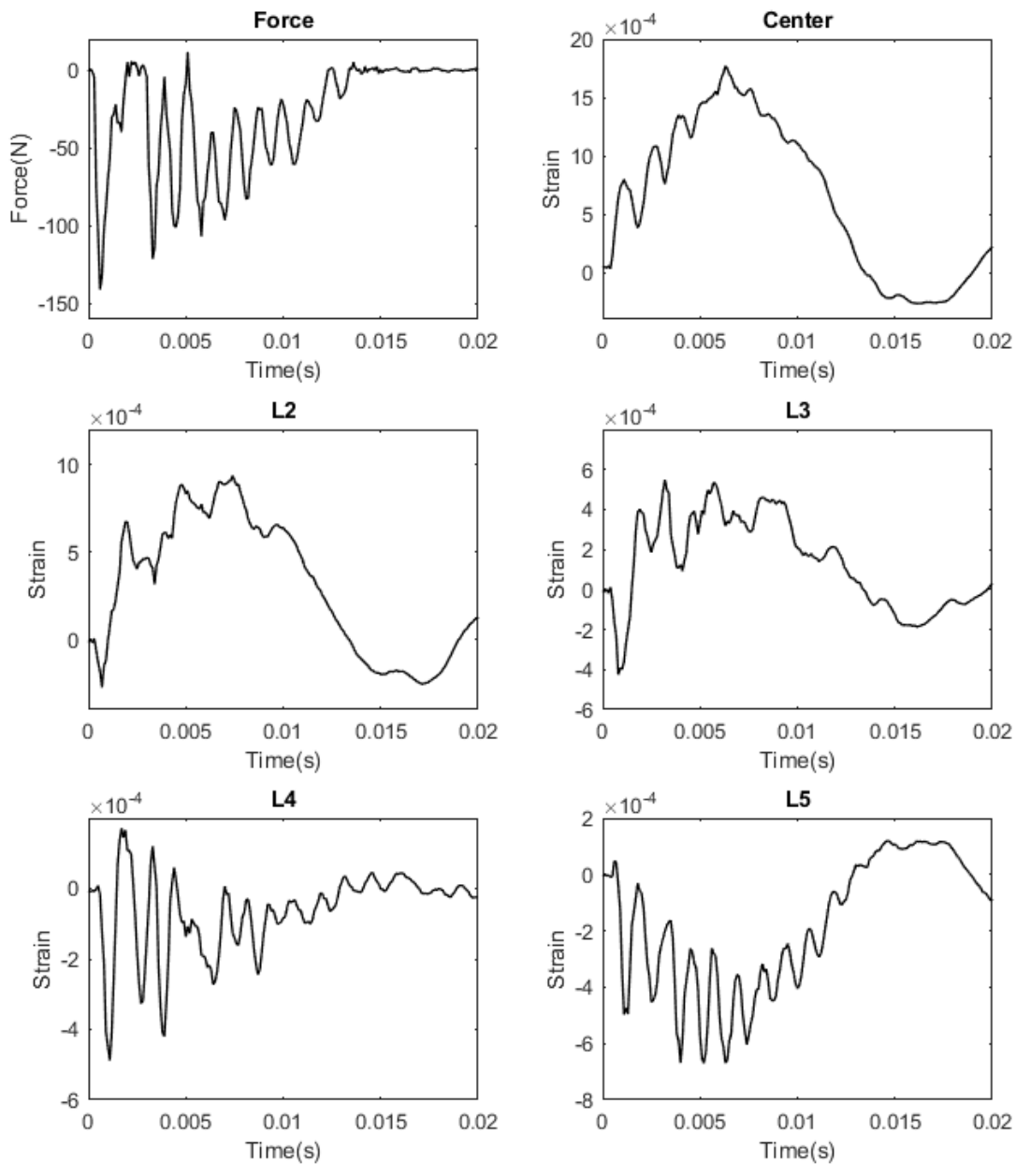


Figure 6. Impact force and strain plots for the tube with 100% stationary water

1
2
3
4
5
6
7
8
9
10
11
12
13
14
15
16
17
18
19
20
21
22
23
24
25
26
27
28
29
30
31
32
33
34
35
36
37
38
39
40
41
42
43
44
45
46
47
48
49
50
51
52
53
54
55
56
57
58
59
60
61
62
63
64
65

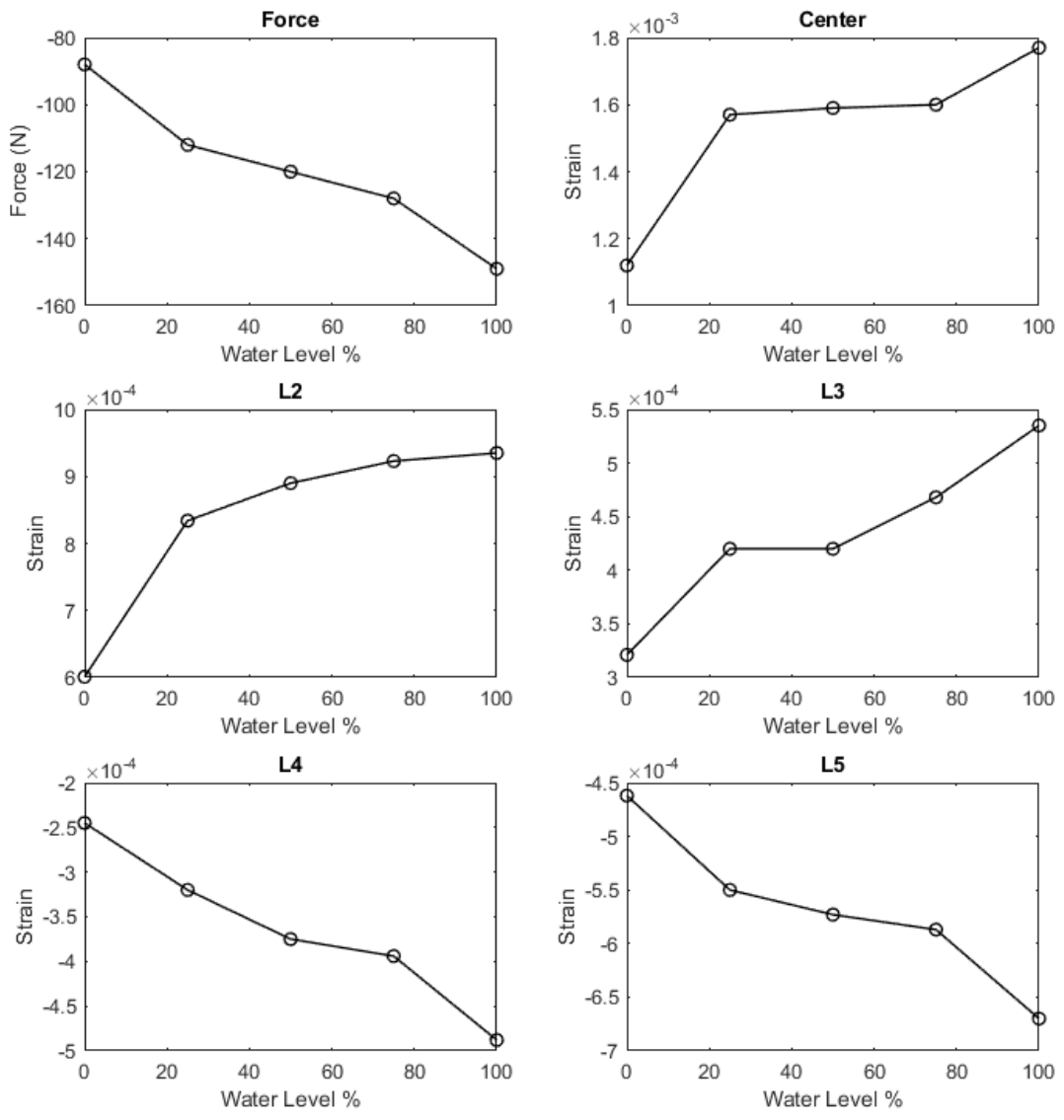


Figure 7. Comparison of maximum values as a function of static water level inside tube

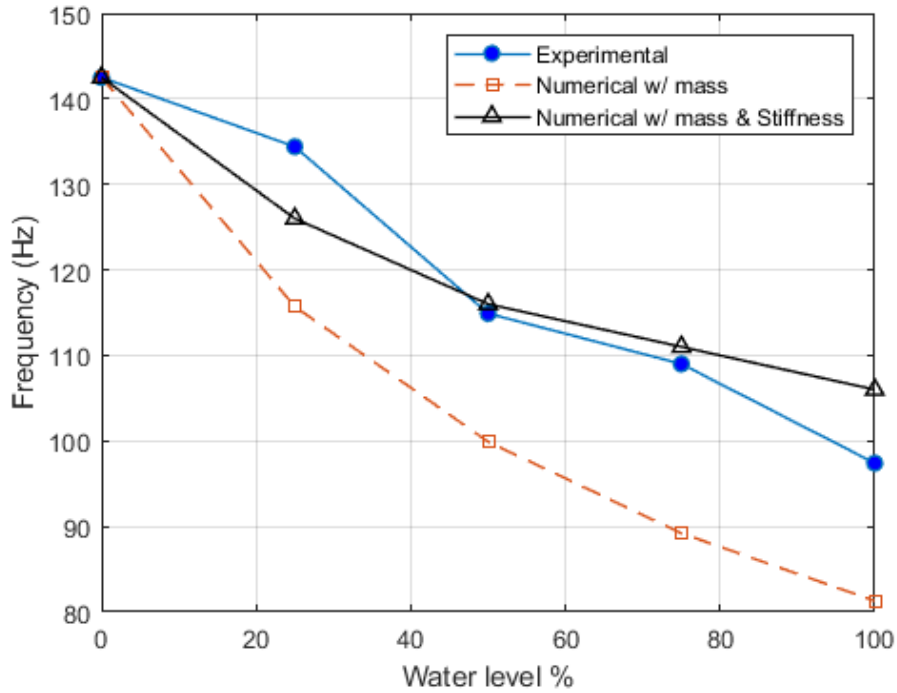


Figure 8. Plot of experimental and numerical frequencies as a function of stationary water level

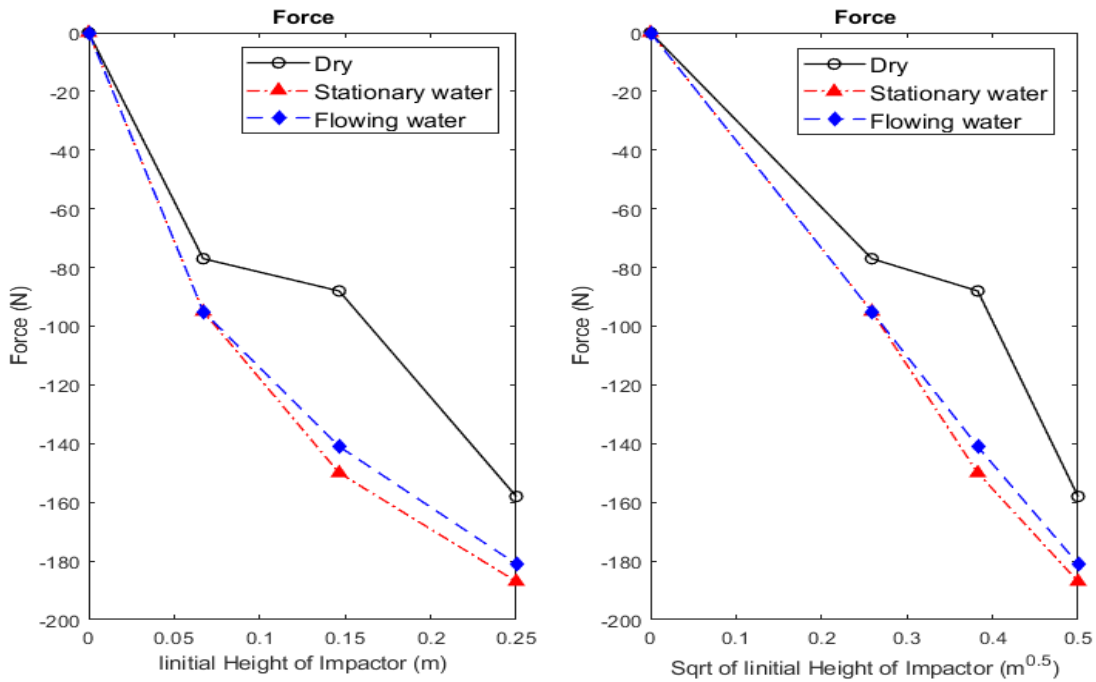


Figure 9. Comparison of peak impact force among tube without water, with 100% full stationary water, and flowing water as a function of the initial impact condition

1
2
3
4
5
6
7
8
9
10
11
12
13
14
15
16
17
18
19
20
21
22
23
24
25
26
27
28
29
30
31
32
33
34
35
36
37
38
39
40
41
42
43
44
45
46
47
48
49
50
51
52
53
54
55
56
57
58
59
60
61
62
63
64
65

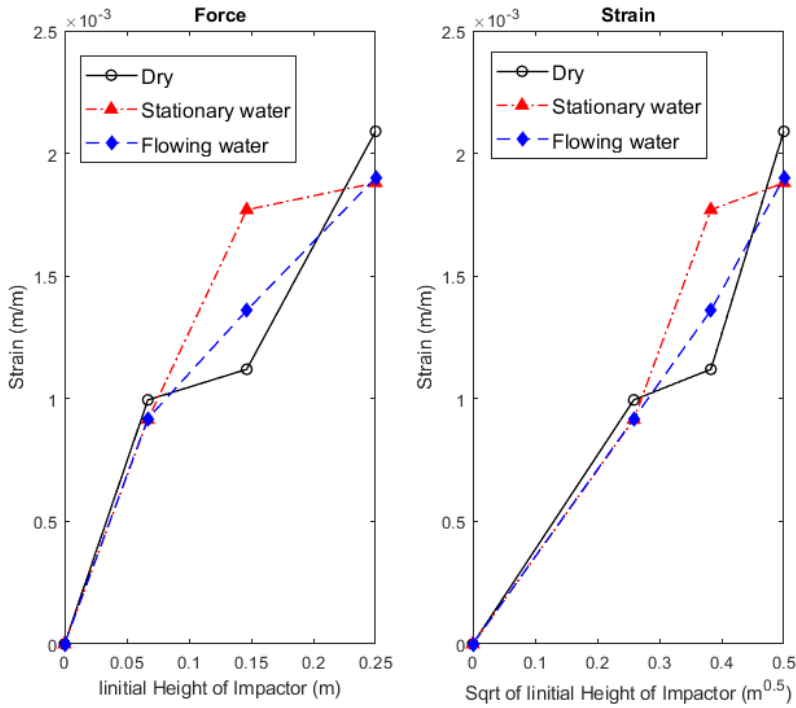


Figure 10. Comparison of maximum strain at the center among tube without water, with 100% full stationary water, and flowing water as a function of the initial impact condition

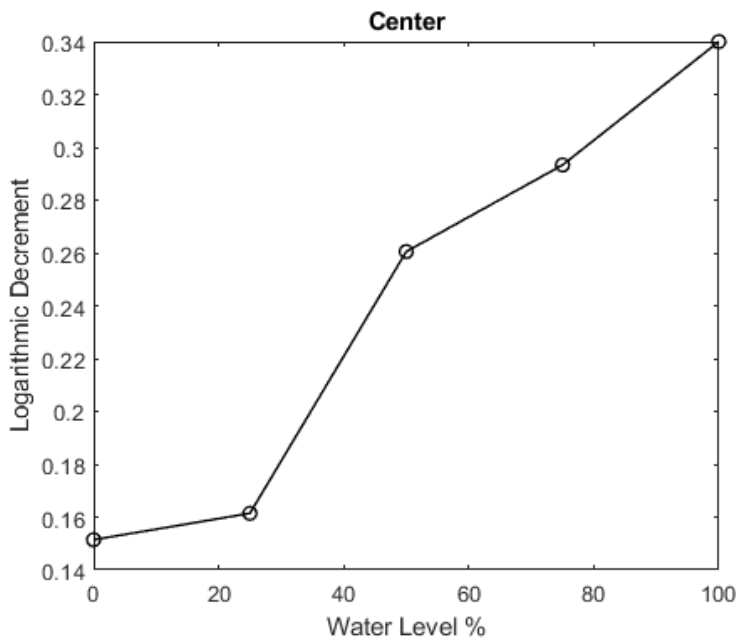


Figure 11. Plot of logarithmic decrement as a function of stationary water level